Published September 20, 2010

n = 5; 7 d post-stimulation: WT-SCF-Fx, 34.1 ± 1.4 vs. WT-PBS-Fx, 12.9 ± 3.3 and WT-SCF-sKit-Fx, 8.0 ± 1.0 × 10^4 cells/ml, P < 0.01, n = 5, [Lnk KO-sKit-Fx, 22.1 ± 3.4 × 10^4]; 14 d post-fracture: WT-SCF-Fx, 17.9 ± 2.0 vs. WT-PBS-Fx, 8.5 ± 1.9 and WT-SCF-sKit-Fx, 7.7 ± 1.3 × 10^4 cells/ml, P < 0.05, n = 5, [Lnk KO-sKit-Fx, 15.0 ± 4.8 × 10^4]; Fig.6 c).

We further confirmed that SCF-induced stem/progenitor cell mobilization mediated enhanced angiogenesis and osteogenesis in sites of fracture by SCF–cKit signaling inhibition study in vivo. The mSCF (20 µg/kg/day), sKit (20 µg/kg/day), or PBS was injected intraperitoneally into mice with fracture for 5 d, and angiogenesis/osteogenesis was evaluated by immunofluorescent staining for CD31 and OC 7 d after surgery (Fig. 6 d). As we expected, SCF stimulation significantly increased both $CD31^+$ capillary density (WT-SCF^+/$sKit^-$, 830.4 ± 55.7 vs. WT-SCF^-/$sKit^-$, 578.6 ± 55.2/mm^2, P < 0.05, n = 5; Fig. 6 e) and OC^+ OB density (WT-SCF^+/$sKit^-$, 495.8 ± 52.2 vs. WT-SCF^-/$sKit^-$, 350.0 ± 25.8/mm^2, P < 0.05, n = 5; Fig. 6 f) around the endochondral ossification area compared with PBS injection (control: SCF^-/$sKit^-$) in WT mice, and the effect of SCF on the increase of capillary density (WT-SCF^+/$sKit^+$, 601.8 ± 60.0 vs. WT-SCF^+/$sKit^-$,

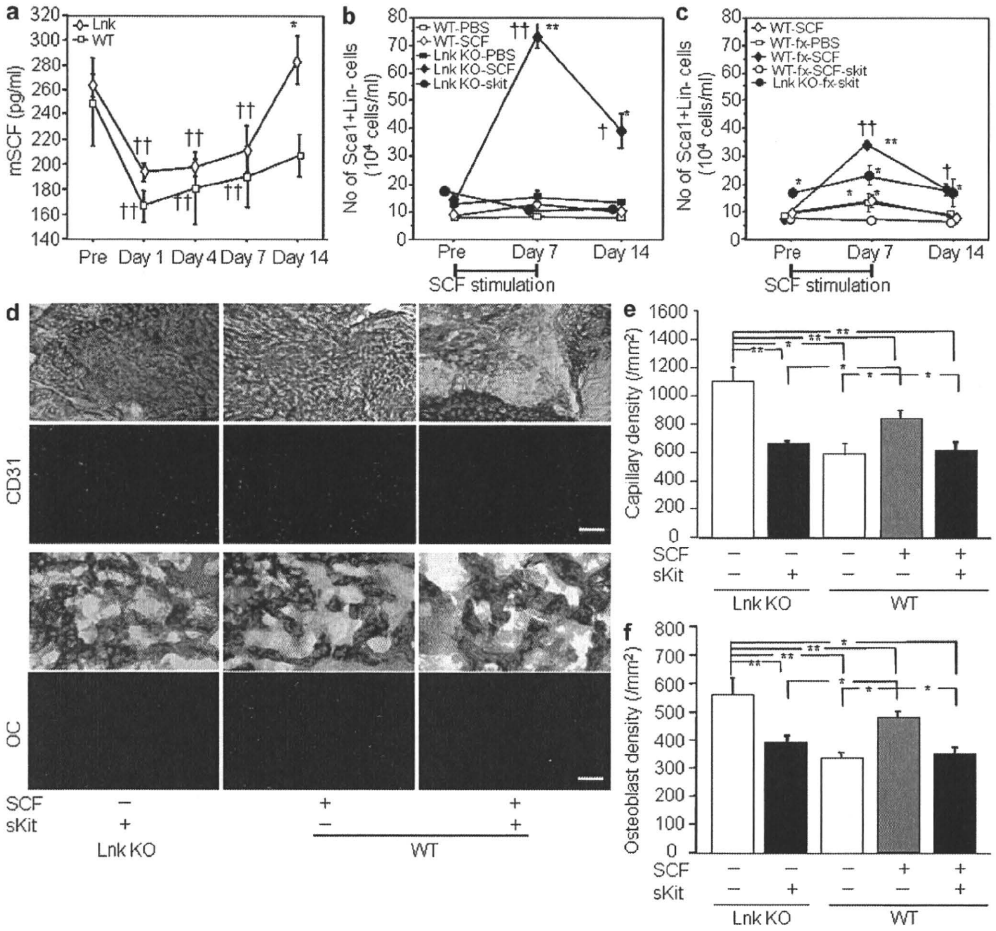

Figure 6. Enhanced SL cell mobilization by SCF stimulation in Lnk KO mice. (a) Serum mouse SCF levels were measured in Lnk KO and WT mice after fracture by ELISA. ††, P < 0.01; *, P < 0.05 versus Pre, respectively. (b) The number of circulating SL cells in Lnk KO and WT mice with injection of PBS (control; Lnk KO-PBS and WT-PBS), SCF (SCF, 20 µg/kg; Lnk KO-SCF and WT-SCF), or soluble SCF receptor (=c-kit ligand, sKit, 20 µg/kg; Lnk-sKit) were assessed by FACS in the indicated time course after the treatment. †† and †, P < 0.01 and P < 0.05 versus Pre, respectively. ** and *, P < 0.01 and P < 0.05 versus WT-PBS, WT-SCF, Lnk KO-PBS, and Lnk KO-sKit, respectively. (c) The number of circulating SL cells in WT mice with fracture and injection of PBS, SCF (20 µg/kg), or SCF (20 µg/kg)+ sKit (WT-fx-PBS, WT-fx-SCF, or WT-fx-SCF-sKit, respectively), WT mice without fracture and SCF (20 µg/kg; WT-SCF), and Lnk KO mice with fracture and sKit (Lnk KO-fx-sKit) were assessed by FACS in the indicated time course after the treatment. †† and †, P < 0.01 and P < 0.05 versus Pre, respectively. * and **, P < 0.05 and P < 0.01 versus WT-fx-SCF-sKit, respectively. (d) Immunofluorescent staining for CD31 (green) and OC (OC, green) were performed in granulation tissue samples of peri-fracture sites in Lnk KO (left one panel) and WT (right two panels) mice 7 d after fracture. Alcian blue/orange G stained sections were also shown in parallel with immunostained sections (lower panels to each immunofluorescent staining images). Mouse phenotype with SCF (20 µg/kg) or sKit (20 µg/kg) administration (+) is indicated in the lower part of images. Dotted line indicates bone surface. Bar = 50 µm. Quantification of capillaries (e) and OBs (f). CD31 positive capillaries and OC positive OBs were counted in 3 randomly selected high power fields and averaged.**, P < 0.01 and *, P < 0.05. All data averaged with SEM from five independent experiments. All experiments were obtained from triplicated assays.

Published September 20, 2010

830.4 ± 55.7/mm², P < 0.05, *n* = 5; Fig. 6 e) and OB density (WT-SCF⁺/sKit⁺, 344.6 ± 20.7 vs. WT-SCF⁺/sKit⁻, 495.8 ± 52.2/mm², P < 0.05, *n* = 5; Fig. 6 f) was significantly reversed by coadministration of sKit with SCF. The sKit administration also significantly reduced both capillary density (Lnk KO-SCF⁻/sKit⁺, 653.6 ± 20.4 vs. Lnk KO-SCF⁻/sKit⁻, 1,101.8 ± 97.7/mm², P < 0.01, *n* = 5; Fig. 6 e) and OB density (Lnk KO-SCF⁻/sKit⁺, 389.3 ± 17.3 vs. Lnk KO-SCF⁻/sKit⁻, 558.9 ± 37.9/mm², P < 0.01, *n* = 5; Fig. 6 f) in Lnk KO mice to levels similar to those found in WT mice with or without coadministration of SCF and sKit. These findings indicate that enhanced SL cell mobilization into PB and its recruitment to fracture sites in Lnk KO mice is, at least in part, regulated by SCF–cKit signaling pathway.

SCF–cKit signaling-dependent terminal differentiation of Lnk-deficient OBs for osteogenesis

Although there is no doubt about stimulated stem/progenitor cell recruitment to sites of fracture by SCF–cKit signaling activation in WT and Lnk KO mice, the Lnk-regulated differential potential of progenitors needed to be evaluated, especially regarding osteogenesis. We isolated mouse calvarial OBs from 3–5-d-old Lnk KO mice and WT mice, and compared the differentiation capacity in osteogenic condition medium after 7, 14, and 21 d in culture. Alkaline phosphatase (ALP) staining exhibited larger nodule formation in Lnk KO OBs than in WT OBs until day 14 (Fig. 7 a). In addition, OB mineralized matrix formation assessed by alizarin red staining in Lnk KO OBs was striking compared to that in WT OBs (Fig. 7 a). Quantitative analysis for calcium content in culture medium was also significantly high in Lnk KO OBs than that in WT OBs after 21 d in culture, (Lnk KO-SCF⁻/sKit⁻, 15.9 ± 3.5 vs. WT-SCF⁻/sKit⁻, 0.6± 0.1 mg/ml, P < 0.01, *n* = 5; Fig. 7 d). However, the number of OB CFUs (CFU-O) showed no statistical differences between the two groups at each time point (unpublished data).

Next, we investigated whether this enhancement of differentiation and mineralized matrix formation in Lnk KO OBs was also regulated by SCF signals. First, we confirmed the significantly higher mRNA expression of SCF in Lnk KO mice than that in WT OBs by real-time RT-PCR analysis (Lnk KO, 1.707 ± 0.345 vs. WT, 0.587 ± 0.111, P < 0.05, *n* = 3; Fig. 7 b). In WT mice, as we expected, SCF morphologically enhanced mineralized matrix formation after 21 d in culture (WT-SCF⁺/sKit⁻), and the effect of SCF on WT OBs (WT-SCF⁺/sKit⁺) and Lnk KO OBs (Lnk KO-SCF⁻/sKit⁺) was inhibited by sKit (Fig. 7 c). Calcium content in WT OBs with SCF was significantly higher than that in WT OBs without SCF (WT-SCF⁺/sKit⁻, 7.1 ± 1.4 vs. WT-SCF⁻/sKit⁻, 0.6± 0.1 mg/ml, P < 0.05, *n* = 5), and the effect was reversed by coincubation of SCF and sKit in WT OBs (WT-SCF⁺/sKit⁻, 1.0 ± 0.3 vs. WT-SCF⁺/sKit⁻, 7.1 ± 1.4 mg/ml, P < 0.05, *n* = 5) and in Lnk KO OBs (Lnk KO-SCF⁻/sKit⁺, 4.8 ± 1.1 vs. Lnk KO-SCF⁻/sKit⁻, 15.9 ± 3.5 mg/ml, P < 0.01, *n* = 5; Fig. 7 d). We then further investigated the role of SCF–cKit signaling, focusing on an osteogenesis-related key molecule, bone morphogenetic protein (BMP)-2, was examined in Lnk KO OBs and WT OBs with SCF stimulation in the presence or absence of sKit. The significantly high BMP-2 mRNA expression was observed in Lnk KO OBs and SCF-treated WT OBs compared with WT OBs (Lnk KO-SCF⁻/sKit⁻, 2.732 ± 0.551 and WT-SCF⁺/skit⁻, 2.576 ± 0.369 vs. WT-SCF⁻/skit⁻, 1.189 ± 0.161, P < 0.01, *n* = 3 in each group) and the BMP-2 mRNA up-regulation in Lnk KO OBs and that in SCF-treated WT OBs were significantly inhibited by sKit (Lnk KO-SCF⁻/sKit⁺, 1.391 ± 0.203 vs. Lnk KO-SCF⁻/sKit⁻, 2.732 ± 0.551 and WT-SCF⁻/sKit⁺, 0.911 ± 0.136 vs. WT-SCF⁺/skit⁻, 2.576 ± 0.369, P < 0.01, *n* = 3; Fig. 7 e). These results indicate that BMP-2 might be involved in the SCF–cKit signaling pathway, which is critical for OB terminal differentiation and mineralized matrix formation leading to osteogenesis enhancement in Lnk KO mice.

Lnk gene deficiency in BM cells plays a critical role for fracture healing

Finally, we examined whether Lnk gene deficiency in BM stem/progenitor cells, but not in bone with surrounding tissue. To test this hypothesis, we assessed fracture healing in a murine BMT model. BM cells isolated from either Lnk KO mice or WT mice were transplanted to Lnk KO mice after lethal irradiation, and generated the following chimera mice: 1) Lnk KO mice with Lnk KO BM and 2) Lnk KO mice with WT BM. These chimera mice underwent surgery for fracture and evaluated the fracture healing by micro-CT imaging system and biomechanical analysis 28 d after surgery. The results of micro-CT exhibited striking trabecular bone formation in Lnk KO mice with Lnk KO BM than that in Lnk KO mice with WT BM (Fig. 8 a). Quantitative analysis for bone formation was performed with micro-CT images, and expressed as bone density (Fig. 8 b, left) and trabecula number (Fig. 8 b, right). The both parameters were significantly great in Lnk KO mice with Lnk KO BM compared with that in Lnk KO mice with WT BM (Bone density: Lnk KO mice with Lnk KO BM, 11.3 ± 0.4 vs. Lnk KO mice with WT BM, 8.9 ± 0.8, P < 0.05, *n* = 4 and Number of trabecular: Lnk KO mice with Lnk KO BM, 3.0 ± 0.2 vs. Lnk KO mice with WT BM, 1.8 ± 0.1, P < 0.05, *n* = 4). Biomechanical examinations by three-point bending test also showed significantly increased ultimate stress ratio (Lnk KO mice with Lnk KO BM, 1.1 ± 0.05 vs. Lnk KO mice with WT BM, 0.5 ± 0.08, P < 0.05, *n* = 4), failure energy ratio (Lnk KO mice with Lnk KO BM, 3.9 ± 0.07 vs. Lnk KO mice with WT BM, 1.5 ± 0.05, p<,0.001 *n* = 4), and extrinsic stiffness ratio (Lnk KO mice with Lnk KO BM, 0.8 ± 0.03 vs. Lnk KO mice with WT BM, 0.2 ± 0.03, P < 0.05, *n* = 4; Fig. 8 c). These results suggest that Lnk gene deficiency in BM cells, rather than in bone with surrounding tissue, is critical for enhanced fracture healing.

DISCUSSION

In this paper, we have demonstrated that both vasculogenesis and osteogenesis were enhanced via large-scale HSC/EPC mobilization in circulation and recruitment to sites of fracture,

Published September 20, 2010

simultaneously resulting in accelerated bone healing in a Lnk-deficient mouse fracture model.

BM SL cells, recognized as an HSC/EPC-enriched fraction (Takahashi et al., 1999), were reported to synthesize ALP, collagen, and OC and form a mineralized matrix in culture over a decade ago (Van Vlasselaer et al., 1994). It has also been reported that BM side population cells, which contain hematopoietic repopulating cells, can also engraft in bone after transplantation (Dominici et al., 2004), and that the nonadherent population of BM cells contains primitive cells able to generate both hematopoietic and osteocytic lineage cells (Olmsted-Davis et al., 2003). Zhang et al. (2003) reported that depleting a receptor of BMP in OBs caused a doubling in both OB and HSC populations in BM niche. Calvi et al. (2003) also found a parallel expansion of the HSCs when the number of OBs was increased by parathyroid hormone infusion. These findings indicate that osteogenesis and hematopoiesis/vasculogenesis closely regulated each other in terms of

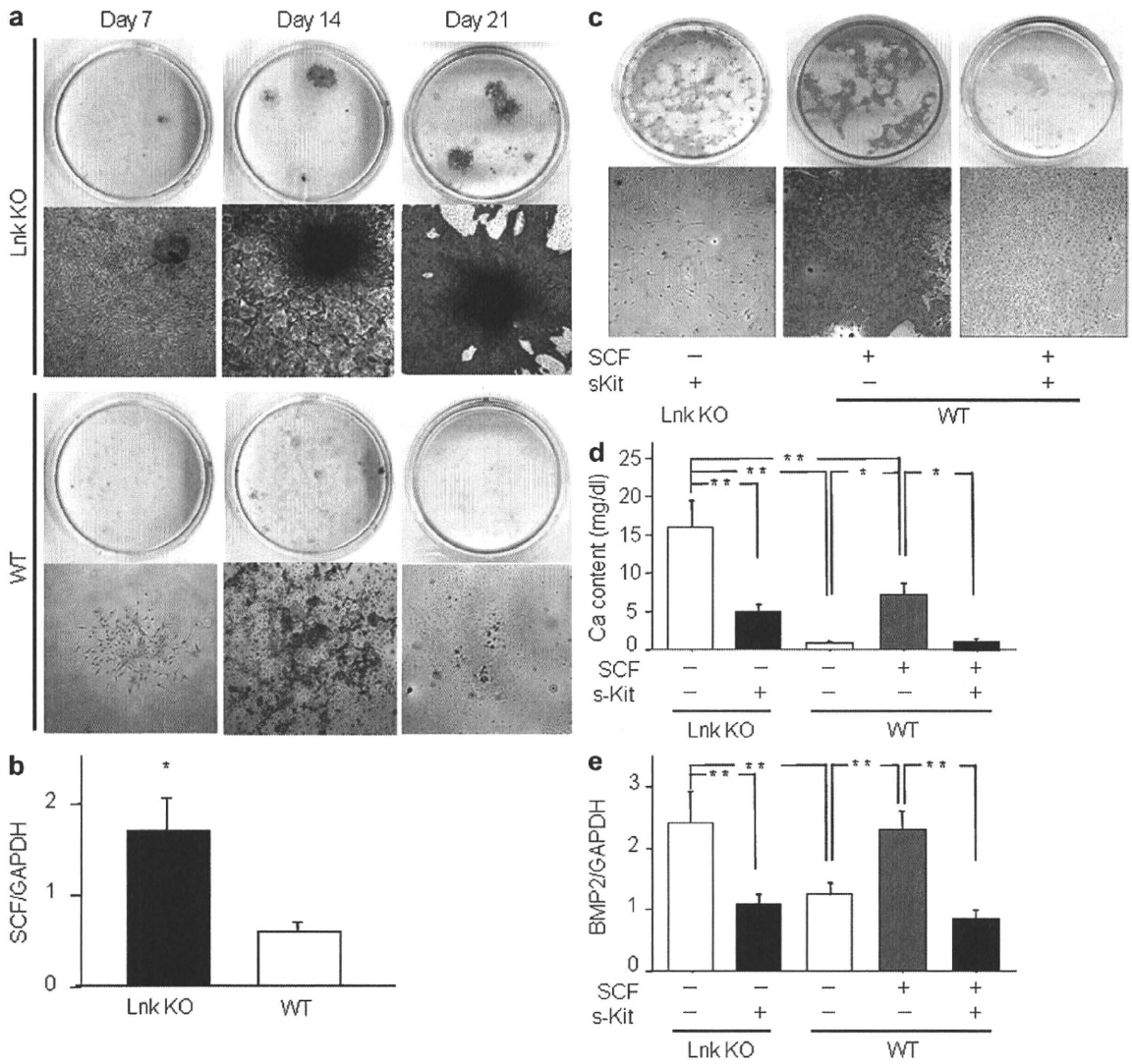

Figure 7. Enhanced mineralization of OBs in Lnk-deficient mice. (a) OBs (OBs) isolated from Lnk KO and WT mice were cultured in osteogenic condition medium. Cells were assessed morphologically by ALP staining (blue) at day 14 and by alizarin red staining (red) at day 21. Upper panels show macroscopic images of whole culture dishes and lower panels show magnified images of nodule with mineralized matrix formation. (b) Real-time RT-PCR of cultured OBs for SCF mRNA expression at day 7 in Lnk KO and WT mice. Mouse heart and bone are used as positive controls for mouse endothelial and bone-related gene detection (not depicted) *, $P < 0.05$. Data averaged with SEM from three independent experiments. Experiments were obtained from triplicated assays. (c) The mineralized matrix formation was assessed by alizarin red staining 21 d after osteogenic culture in Lnk KO OBs with sKit (10 µg/ml) and in WT OBs in the presence of SCF (100ng/ml) with or without sKit (10 µg/ml). Upper panels show macroscopic images of whole culture dishes and lower panels show magnified images of nodule with mineralized matrix formation. Calcium content was measured by ELISA ($n = 5$ each; d) in culture medium and BMP2 mRNA expression (e) was analyzed by real-time RT-PCR ($n = 3$ each) in Lnk KO OBs with sKit (10 µg/ml) and WT OBs in the presence of SCF (100ng/ml) with or without sKit (10 µg/ml). *, $P < 0.05$ and **, $P < 0.01$. Experiments were obtained from triplicated assays.

Published September 20, 2010

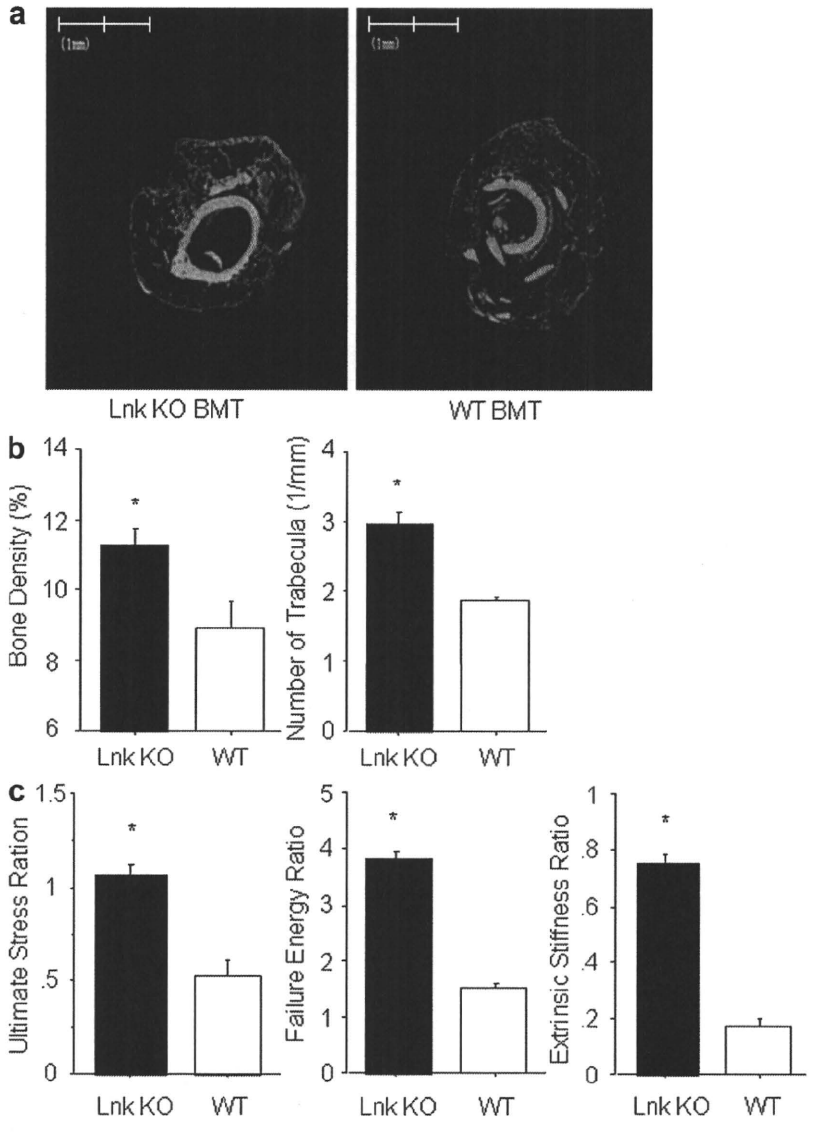

Figure 8. Radiographical and biomechanical function assessment of fracture healing in Lnk KO BMT–Lnk KO mice and WT BMT– Lnk KO mice. (a) The bone structure after healing was assessed by micro-CT 28 d after surgery. (b), Bone density and number of trabecular bones were quantified in the micro-CT images and averaged. *, $P < 0.05$ versus Lnk KO-BMT, $n = 4$ each. (c) Biomechanical function test for healed bone was also assessed 28 d after fracture. Each parameter, ultimate stress (left), fracture energy (center) and extrinsic stiffness ratio (right), was evaluated as healed bone function. *, $P < 0.05$ and **, $P < 0.001$ versus Lnk KO-BMT. All data averaged with SEM from four independent experiments.

microenvironmental interaction for regenerative activity in BM. We have also previously reported that mobilization of BM-derived HSCs/EPCs were triggered by fracture onset and recruited to sites of fracture (Matsumoto et al., 2008). In this study, we have provided evidence of enhanced translineage differentiation of $Sca1^+/Tie2^+$ cells into OBs and ECs both in vitro and in vivo, as well as that of mobilization of BM-KSL cells and PB-SL cells in circulation in Lnk-deficient mice, which is consistent with the previous report that BM cells of Lnk-deficient mice are competitively superior in hematopoietic population to those of WT mice (Takaki et al., 2002). These data suggest that a large number of BM-derived EPCs might not only be mobilized from BM but also recruited to fracture site, differentiating into ECs and OBs by lack of Lnk signaling. In addition to the direct contribution of recruited EPCs for fracture repair, indirect contribution of EPCs, i.e., the paracrine effect on bone tissue regeneration via promotion of osteogenesis/angiogenesis with resident cells, would also be critical for fracture healing (Matsumoto et al., 2006). Indeed, cDNA microarray and quantitative real-time RT-PCR analyses also exhibited up-regulation of pro-angiogenic/-osteogenic gene expressions, which is consistent with increased blood perfusion and callus formation, in sites of fracture with recruited EPCs in Lnk-deficient mice. The series of findings suggest that both direct and indirect contribution of BM-derived EPCs to prompt and functional fracture healing with sufficient mineralization in Lnk-deficient mice.

Takaki et al. (2000, 2002) reported that Lnk acts as a negative regulator in the SCF–cKit signaling pathway. Although the role of Lnk system has gradually been clarified in the field of hematology, nothing is known about it's role in skeletal biology and bone regeneration and repair. Here, we have provided evidence that enhanced HSC/EPC mobilization into PB and its recruitment to the fracture site in Lnk-deficient mice are regulated, at least in part, by SCF–cKit signaling pathway, which was proved by gain and loss of function test using SCF and sKit. However, enhanced vasculogenesis and osteogenesis in Lnk-deficient mice was shown to be significantly superior to that of SCF-treated WT mice, suggesting that another mechanism besides SCF–cKit signaling pathway is involved in the Lnk signal lacking accelerated bone healing. Indeed, molecular cDNA array analysis showed that BMPR2 mRNA expression was up-regulated more in Lnk KO mice than in WT mice. Moreover, lack of Lnk or SCF supplement in OBs induced terminal differentiation and mineralized matrix formation with increased BMP2 gene expression, which was blocked by the SCF antagonist sKit. These findings are consistent with previous studies in which cKit expression is shown in OBs and P-2 enhances OB differentiation. (Bilbe et al., 1996; Hassel et al., 2006) Collectively, it is suggested that OB differentiation and maturation is enhanced in Lnk-deficient mice via the mechanism of BMP2-involved SCF–cKit signaling pathway.

Published September 20, 2010

Another interesting finding in cDNA microarray data is that expression of vascular cell adhesion molecule (VCAM)-1, a differentiation-predicting marker for osteogenesis (Fukiage et al., 2008), is significantly up-regulated in sites of fracture and EC-related markers in Lnk KO mice compared with WT mice. Fitau et al. (2006) reported that high expression of VCAM-1 at both the mRNA and protein level in Lnk-deficient mice was regulated in TNF-treated ECs by extracellular signal-related kinase (Erk) 1/2 pathways. In addition, Rhee et al. (2006) reported that Erk 1/2 expression was present within mesenchymal precursor cells during distraction osteogenesis and that Erk expression closely correlates with BMP 2/4 expression. Other studies also indicated that the activation of Erk 1/2 pathway in OBs related to mechanical strain and fluid flow (Jessop et al., 2002; Alford et al., 2003; Liu et al., 2008). Based on this evidence and our findings, the Erk1/2- and BMP-2/4–involved VCAM-1 signaling pathway is considered to be another mechanism for accelerated fracture healing via vasculogenesis and osteogenesis in Lnk KO mice, and further investigation will be required to clarify the entire mechanism for bone regeneration in a Lnk-deficient system.

In conclusion, our data provide novel evidence that the Lnk system acts as a negative regulator in the SCF–c-Kit signaling pathway and that Lnk deficiency modulates both vasculogenesis and osteogenesis via SL stem cell mobilization in PB and Tie2$^+$ BM cell recruitment to sites of fracture, although Tie2$^+$ cells are not necessarily defined as stem cells, but are likely EPCs. In addition, lack of Lnk signaling further enhances BMP2-induced OB matrix mineralization in vitro. These pathophysiological changes led to accelerated bone healing in Lnk-deficient mice. In the field of skeletal regeneration, recently BM-derived mesenchymal stem cells or whole BMs have been used for injured bone (Petite et al., 2000) or osteogenesis imperfecta (Horwitz et al., 1999) in preclinical studies. However, there are several issues to be resolved for open reduction, such as invasiveness in cell transplantation procedure and possible complications caused by infection. The major strength of this study relies on the concept that negative control of Lnk system for bone regeneration leads to clinical feasibility by generating a Lnk-inhibitory compound. This is the first study demonstrating physiological functions of the adaptor protein Lnk in bone regeneration and suggests that inhibition of the Lnk system could be a novel therapeutic application for genetic bone diseases and bone injuries.

MATERIALS AND METHODS

Mice. Lnk$^{-/-}$ mice, whose generation and genomic cloning were described previously (Takaki et al., 2000) were backcrossed with C57BL/6 (B6-Ly5.2) >10 times and paired with age-matched WT mice as controls. Mice congenic for the Ly5 locus (B6-Ly5.1) were bred and maintained at the animal facility of Institute of Physical and Chemical Research Center for Developmental Biology, Kobe, Japan. The mice were fed a standard maintenance diet and provided water ad libitum. Male 10–12-wk-old Lnk$^{-/-}$ and WT mice were used in this study. The institutional animal care and use committees of the Institute of Physical and Chemical Research Center for Developmental Biology approved all animal procedures, including human cell transplantation.

Isolation of Lin$^-$ BM cells. To confirm the kinetics of KSL or SL cells in BM and PB, we detected KSL or SL cells at pre-fracture and 1, 4, 7, and 14 d post-fracture by FACS analysis (n = 3 at each day).

BM cells were obtained by flushing femurs and tibiae or PB cells were aspirated from the hearts of 10-wk-old Lnk KO mice or WT mice with PBS containing 5% FCS. MNCs were obtained by gradient separation onto a Ficoll Histopaque gradient. Separation of Lin$^-$ cells was performed by labeling MNCs with a lin$^-$ separation kit (BD) containing biotin-conjugated Mac1, B220, CD3e, Ter119, Ly6G, and CD45R antibodies, followed by streptavidin-conjugated magnetic beads and BD IMagnet separation before Lin$^-$ MNCs were counted.

Multilineage differentiation culture of SL BM cells. Mouse SL cells were isolated from BM MNCs by Lin$^+$ cell depletion with MACS system (Miltenyi Biotec) followed by FACS system with an anti–mouse Sca-1 antibody (FACSAria; BD), and cultured in α-modified Eagle's medium (α-MEM; Cambrex Bio Science). After 3 wk in culture, cells (10^5/well) were placed in a 6-well plate and further cultured only for osteogenic and adipogenic induction.

For endothelial induction, freshly isolated SL cells were cultured in EBM-2 medium supplemented with 10% FBS and EGM-2 Bullet kit (Lonza) in Pronectin F (Sanyo Chemical, Inc.)–coated culture plate for 7 d. For osteogenic and adipogenic induction, cells were cultured in α-MEM supplemented with 10% FBS. 2 mM L-glutamine, 60 μM ascorbic acid, 10 mM β-glycerophosphate and 0.1 μM dexamethasone (Sigma-Aldrich) and α-MEM supplemented with 1 μM dexamethasone, 60 μM indomethacin, and 5 μg/ml insulin (Sigma-Aldrich) for 3 wk, respectively. After the above induction cultures, each lineage differentiation was confirmed by real-time RT-PCR and fluorescent immunocytostaining for the indicated specific markers. Also, calcium deposits were detected by Alizarin red staining and formations of lipid droplets were assessed by Oil Red O staining as characteristics of OB and AD, respectively. Freshly isolated SL cells and those cultured for 3 wk in α-MEM alone were used as controls for endothelial induction and osteogenic/adipogenic induction in real-time RT-PCR analysis, respectively.

Flow cytometry studies and monoclonal antibodies. Regular flow cytometric profiles were analyzed with a FACSCalibur analyzer and CELLQuest software (BD). The instrument was aligned and calibrated daily using a four color mixture of CaliBRITE beads (BD) with FACSComp software (BD). Dead cells were excluded from the plots beads on propidium iodide (PI) staining (Sigma-Aldrich). Lineage-depleted MNCs were washed twice with HBSS containing 3.0% heat-activated FCS, and incubated with 10 μl of FcR Blocking Regent to increase the specificity of monoclonal antibodies (Miltenyi Biotec) for 20 min at 4°C, and incubated with the monoclonal antibodies for 30 min at 4°C. The stained cells were washed three times with PBS containing 3.0% FCS, and resuspended in 0.5 ml of HBSS/3%FCS/PI, and analyzed by FACScan caliber flow cytometer (BD). The following monoclonal antibodies were used to characterize the lineage-depleted MNCs: APC-conjugated anti-cKit (BD), FITC-conjugated anti-Sca1 (BD), IgG1-PE isotype controls (BD), IgG1-FITC isotype controls (BD), and PI (Sigma-Aldrich).

Induction of femoral fracture. All surgical procedures were performed under anesthesia and normal sterile conditions. Anesthesia was performed with ketamine hydrochloride (60 mg/kg) and xylazine hydrochloride (10 mg/kg) administered intraperitoneally. We followed Manigrasso's model of closed femur fracture (Manigrasso and O'Connor, 2004). A lateral parapatellar knee incision on the right limb was made to expose the distal femoral condyle. A 2-mm wedge was made using a 27-gauge needle on the intercondyle of the femur and then a 0.5-mm-diam, stainless wire was inserted in a retrograde fashion. The wire was advanced until its proximal end was positioned stable to the greater trochanter and the distal end was cut close to the articular surface of the knee. A transverse femoral shaft fracture was then created in the right femur of each mouse by three-point bending. The wound was then irrigated with 10 cc of sterile saline and skin was closed in layers with 5–0

Published September 20, 2010

nylon sutures. Postoperative pain was managed by administration of subcutaneous injection of buprenorphine hydrochloride after surgery. Unprotected weight bearing was allowed immediately after the operation. The left nonfractured femur served as a control.

20 animals were assigned to each group for radiological assessment, and every additional three to five animals in each group were assigned for each study. If the fracture produced was not a stable transverse fracture or if evidence of deep infection developed then animals were excluded from the study and replaced with another animal. Thus, six mice with comminuted fractures were replaced during the experiment. No mice developed infections, as confirmed by radiograph.

Mouse BMT model. Male Lnk KO mice and WT mice (C57BL6/J; CLEA Japan, Inc.) aged 6 wk were used as recipients for BMT. Transgenic mice of B6/N-TgN (Tie-2-LacZ)^{182Sato} (Jackson ImmunoResearch Laboratories), which were generated by backcrossing FVB/N-TgN (Tie-2-LacZ)^{182Sato} mice and C56BL6/J mice, were used as donors for the BMT. The procedure of BMT was performed as described previously, with some modifications (Ii et al., 2005). In brief, the recipient mice were lethally irradiated for BM ablation with 12.0 Gy and received 5 million donor BM MNCs. At 4–6 wk after BMT, by which time the BM of the recipient mice was reconstituted, surgery for fracture induction was performed. The granulation tissue of fractured BMT mice were harvested 7 and 28 d after surgery for histological, radiographical, and biomechanical function analyses.

Gene expression analysis via cDNA microarray. Total RNA was obtained from tissues at the peri-fracture site at day 7 using Tri-zol (Life Technologies) according to the manufacturer's instructions. cDNAs were synthesized using 1 μg total RNA in the presence of Superscript II and Oligo $(dT)_{1218}$ (both from Invitrogen). PCR was performed in a 20-μl reaction solution containing 2 μl 10 X PCR buffer, 150 nmol $MgCl_2$, 10 nmol dNTP, 20 pmol primer, 1 μl 10× diluted cDNA, and 1 U RedTag DNA polymerase (Sigma-Aldrich). PCRs were run as follows: 35 cycles of 94°C for 30 s, 55°C for 30 s and 72°C for 30 s, and a final extension for 10 min at 72°C. Primer sequences are shown in the Primer size and sequence section. Nonradioactive GEArray Q series cDNA expression array filters (Mouse Angiogenesis Gene Array [MM-009] and Mouse Osteogenesis Gene Array [MM-026]; SuperArray Inc.) were used to perform focused array analysis as described by the manufacturer. Microarray databases are available at the National Center for Biotechnology Information Gene Expression Omnibus (GEO; http://www.ncbi.nlm.nih.gov/geo/) under accession no. GPL1121 for MM-009 and GPL1143 for MM-026. In brief, biotin dUTP-labeled cDNA probes were generated in the presence of a designed set of gene-specific primers using total RNA (2 μg per filter) and 200 U MMLV reverse transcription (Promega, Madison, WI, USA). The array filters were hybridized with biotin-labeled probes at 60°C for 17 h. Filters were first washed twice with 2× saline sodium citrate buffer (SSC)/1% sodium dodecyl sulfate (SDS) and then twice with 0.1× SSC/1% SDS at 60°C for 15 min each. Chemiluminescent detection steps were performed by subsequent incubation of the filters with ALP-conjugated streptavidin and CDP-Star substrate. The images were captured using ChemoFlure 8900 (Alpha Innotech). For data analysis, positive and negative spots were independently identified and verified by at least two people. Only matched positive and negative results from two independent experiments were used for analysis. For quantification, intensity of spots was first measured by National Institutes of Health image software (ImageJ) and then the mean intensities derived from the blank spots were subtracted. These subtracted intensities were divided by the mean intensities from GAPDH (three spots in each array), to obtain a relative intensity for each spot. These relative intensities were used to compare gene express levels between the control and the stimulated groups.

Real-time quantitative RT-PCR analysis of RNA isolated from peri-fracture site and cultured OBs. Total RNA was obtained from tissues of peri-fracture site at day 7 or from cultured OBs using TRIzol (Life Technologies) according to the manufacturer's instructions. After total RNA isolation, we made single-strand cDNA using a reverse transcription kit (Invitrogen) and used it as template for real-time PCR with SYBR Green PCR Master Mix (Applied Biosystems) and gene-specific primers in an Oligo software (Takara Bio Inc.). The mean cycle threshold values from quadruplicate measurements were used to calculate the gene expression, with normalization to GAPDH as an internal control.

Primer size and sequences. mCD31 (224 bp): sense 5′-TCCCCACCGAAAGCAGTAAT-3′; antisense 5′-CCCACGGAGAAGTACTCTGTCTATC-3′, mVE-cad (369 bp): sense 5′-GAGCTAAGAGGACCCTCTGCTACTC-3′; antisense 5′-TGGGCCTCTTTGTGTCTGTATG-3′, mFlk-1 (346 bp): sense 5′-TGGCGTTTCCTACTCCTAATGA-3′; antisense 5′-GAAGCCACAACAAAGCTAAAATACTGAG-3′, mvWF (20 bp): sense 5′-ACGCCATCTCCAGATTCAAG-3′; antisense 5′-AAGCATCTCCCACAGCATTC-3′, mOC (187 bp): sense 5′-CTGACCTCACAGATCCCAAGC-3′; antisense 5′-TGGTCTGATAGCTCGTCACAA-3′, mCol1A1 (107 bp): sense 5′-CAATGGTGAGACGTGGAAAC-3′; antisense 5′-GGTTGGGACAGTCCAGTTCT-3′, mCbfa1 (151 bp): sense 5′-AACGATCTGAGATTTGTGGGC-3′; antisense 5′-CCTGCGTGGGATTTCTTGGTT-3′, mLPL (65 bp): sense 5′-AGCTGGGAGCAGAAACTGTG-3′; antisense 5′-CATGTGGGTTGGTGTTCAGA-3′, mPPARγ (50 bp): sense 5′-CTGGCCTCCCTGATGAATAA-3′; antisense 5′-AATCCTTGGCCCTCTGAGAT-3′, mSCF (72 bp): sense 5′-CCAAAAGCAAAGCCAATTACAAG-3′; antisense 5′-AGACTCGGGCCTACAATGGA-3′, mBMP-2 (73 bp): sense 5′-TCACTTATAGCCGCATTATCTTCTTC-3′; antisense 5′-TTGGTTTATCCATGAGGCTAACTG-3′, and mGAPDH (484 bp): sense 5′-GTGAGGCCGGTGCTGAGTATG-3′; antisense 5′-AGGCGGCACGTCAGATCC-3′.

Tissue harvesting. Mice were euthanized with an overdose of ketamine and xylazine. Bilateral femurs were harvested and embedded in OCT compound, snap frozen in liquid nitrogen, and stored at −80°C for histochemical staining and immunohistochemistry. Rat femurs in OCT blocks were sectioned, and 6-μm serial sections were collected on slides, followed by fixation with 4.0% paraformaldehyde at 4°C for 5 min, and then stained immediately.

Morphometric evaluation of capillary and OB density. Immunohistochemical staining with anti–mouse rat CD31 (Biogenesis) for mouse EC marker or anti–mouse goat OC (Santa Cruz Biotechnology, Inc.) for mouse OB was performed. The secondary antibodies for each immunostaining are as follows: FITC-conjugated anti–rat IgG (H+L; Jackson ImmunoResearch Laboratories) for CD31 and FITC-conjugated anti–goat IgG (H+L; Jackson ImmunoResearch Laboratories) for OC. Capillary or OB density was morphometrically evaluated by histological examination of 5 randomly selected fields of tissue sections recovered from segments of soft tissue in the peri-fracture site. Capillaries were recognized as tubular structures positive for CD31. OB-like cells were recognized as lining or floating cells positive for OC on new bone surface. All morphometric studies were performed by two examiners who were blinded to treatment.

LDPI assessment. LDPI (Moor Instrument; Wardell et al., 1993; Linden et al., 1995) was used to record serial blood flow measurements over the 3 wk post-fracture course. In these digital color-coded images, red hue indicated regions with maximum perfusion; medium perfusion values are shown in yellow; lowest perfusion values are represented as blue. This was done under anesthesia with the animal supine and both limbs fully fixed.

Fluorescent immunostaining. To detect $Tie2^+$ cell-derived neovascularization in Lnk KO mice with Tie2/LacZ Lnk KO BM at the fracture site, double immunohistochemistry was performed with anti–mouse rat CD31 (1:50; BD) or anti–mouse goat OC (1:250; Biogenesis) and anti–rabbit β-gal (1:1,000; Cortex) to detect $Tie2^+$ cell-derived ECs or OBs. For characterization of multilineage cell types in SL cells, the following primary antibodies were used: anti–mouse rat CD31 (1:50; BD), anti–mouse goat vWF (1:100; Santa Cruz Biotechnology, Inc.), anti–mouse rat Flk-1 (1:100; Chemicon), anti–mouse goat OC (1:250; Biogenesis), and anti–mouse mouse adiponectin

Published September 20, 2010

(1:250; Abcam). The secondary antibodies (1:1,000) for each immunostaining are as follows: FITC-conjugated anti-rat IgG (H+L; Jackson ImmunoResearch Laboratories) for CD31 and Flk-1, FITC-conjugated anti-goat IgG (H+L; Jackson ImmunoResearch Laboratories) for OC and vWF, Alexa Fluor 594–conjugated rabbit anti-mouse IgG (H+L) for adiponectin, and Cy3-conjugated goat anti-rabbit IgG (H+L; Jackson ImmunoResearch Laboratories) for β-gal staining. DAPI solution was applied for 5 min for nuclear staining.

Radiological assessment. Radiographs of the fractured legs were serially taken at weeks 0, 1, 2, 3, and 4 after creation of the fracture. This procedure was done under anesthesia with the animal supine and both limbs fully extended. Fracture union was identified by the presence of bridging callus on two cortices. Radiographs of each animal were examined by three observers who were blinded to treatment. To evaluate the fracture healing process, callus formation was monitored radiographically and relative callus areas detected by radiography were quantified with National Institutes of Health image at week 1 in both groups. To evaluate bone remodeling, callus absorption was monitored radiographically and relative callus density was detected by radiography were quantified with ImageJ at week 3 and 4 in all groups.

For quantification of callus/trabecular bone formation, micro-CT imaging analysis was performed 4 wk after fracture surgery in Kureha Special Laboratory. In brief, bone density and number of trabecula in callus area were calculated with CT intensity in scanned images by single energy x-ray absorptiometry method and averaged.

Biomechanical analysis of fracture union. Biomechanical evaluation was performed with mice at week 4 after fracture in Kureha Special Laboratory. In brief, fractured femurs and the contralateral nonfractured femurs were prepared and intramedullary fixation pins were removed before the bending test. The standardized three-point bending test was performed using load torsion and bending tester "MZ-500S" (Maruto Instrument Co., Ltd.). The bending force was applied with cross-head at a speed of 2 mm/minute until rupture occurred. The ultimate stress (n), the extrinsic stiffness (n/mm) and the failure energy ($n \times$ mm) were interpreted and calculated from the load deflection curve. The relative ratio of the fractured (right) femur to nonfractured (left) femur was calculated in each group and averaged.

Histological assessment. Histological evaluation ($n = 3$ in each group) was performed with toluidine blue staining to address the process of endochondral ossification on weeks 1, 2, and 3. The degree of fracture healing was evaluated at week 1, 2, and 3 in each group using a five point scale proposed by Allen et al. (1980). According to this classification system, grade four represents complete bony union, grade three represents an incomplete bony union (presence of a small amount of cartilage in the callus), grade two represents a complete cartilaginous union (well-formed plate of hyaline cartilage uniting the fragments), grade one represents an incomplete cartilaginous union (retention of fibrous elements in the cartilaginous plate), and grade zero indicates the formation of a pseudoarthrosis (most severe form of arrest in fracture repair). All morphometric studies were performed by two orthopedic surgeons who were blinded to the treatment.

ELISA assessment of plasma SCF levels. SCF plasma levels of mouse were measured at prefracture and 1, 4, 7, and 14 d post-fracture in both groups via ELISA kit (R&D Systems) according to the manufacturer's instructions ($n = 3$ in each group).

Effect of SCF stimulation on mobilization of SL cells. Mice were injected intraperitoneally with 20 μg/kg SCF or PBS for 5 d in un-fractured Lnk KO, WT, and fractured WT mice, and mobilization of SL cells to PB was assessed at prefracture, day 7, and day 14 post-stimulation time point by FACS analysis ($n = 5$ in each group). For the other series, SCF or PBS-treated WT mice of femur fracture model were sacrificed at day 7, and tissue samples of the fractured limbs were assessed by capillary and OB density as mentioned in Morphometric evaluation of capillary and OB density.

Mouse calvarial OB culture. Calvarial cells were isolated from 3–5-d-old mice using a modification of the method described by Wong and Cohn (1975). In brief, after removal of sutures, calvariae were subjected to four sequential 15-min digestions in an enzyme mixture containing 0.05% trypsin (Invitrogen) and 0.1% collagenase P (Boehringer Mannheim) at 37°C on a rocking platform. Cell fractions 2–4 were collected, and enzyme activity was stopped by the addition of an equal volume of DME containing 10% FCS, 100 U/ml of penicillin, and 100 μg/ml of streptomycin (Invitrogen). The fractions were pooled, centrifuged, resuspended in DME containing 10% FCS, and filtered through a 70-μm cell strainer. Cells were plated at a density of 10^4 cells/well in 35-mm culture plates in DME containing 10% FCS. The medium was changed 24 h later, and 3 d later cultures were fed again. At 1 wk of culture, the medium was changed to a differentiation medium (α-MEM containing 10% FCS, 50 μg/ml of ascorbic acid, and 4 mM of β-glycerophosphate) and thereafter the medium was changed every 2 d. CFU-O was scored at day 7, 14, and 21 of incubation by in situ observation of plates on an inverted microscope. Effects of SCF and sKit on CFU-O formation and mineralization were also investigated in the above assay. Purified recombinant human SCF and sKit were purchased from R&D Systems and supplemented concentrations of cytokines used for culture were as follows: SCF 100 ng/ml and sKit 10 μg/ml (Nakamura, 2004).

Histochemical analysis of cell cultures. Histochemical staining for ALP was performed at day 7 and 14 using a commercially available kit (Muto-Kagaku) according to the manufacturer's instruction. Mineralization was assessed using alizarin red staining method. In brief, the cultures were rinsed twice with PBS, fixed in 100% ethanol for 30 min, and stained wth 1% alizarin red S (Hartman Leddon Co.) in 0.28% ammonia water for 10 min at room temperature. The stained cell layers were washed, rinsed twice with distilled water, and air-dried.

Matrix/intracellular calcium accumulation. Calcium content was measured by the orthocresolphthalein complexone (OCPC) colorimetric method (Sigma-Aldrich). In brief, cell layers at day 21 were washed with PBS twice, and then incubated with 50 μl of 0.6 N hydrochloric acid overnight at room temperature. Plates were then vortexed and centrifuged for 20 min at 1,600 g at 25°C and 10 μl of sample was added to 100 μl OCPC solution in fresh wells. The plate was incubated at room temperature for 10 min, and then read at 575 nm. Standards were prepared from a $CaCl_2$ solution and the results were expressed in milligram/milliliter per 10,000 seeded cells.

Statistical analysis. All values were expressed as mean ± SEM. Paired Student's t tests were performed for comparison of data before and after fracture. The comparisons among groups were made using the one-way analysis of variance. Post hoc analysis was performed by Fisher's PLSD test. A p-value < 0.05 was considered to denote statistical significance.

The authors state that there is no conflict of interest.

Submitted: 16 February 2010
Accepted: 30 July 2010

REFERENCES

Ahmed, Z., and T.S. Pillay. 2003. Adapter protein with a pleckstrin homology (PH) and an Src homology 2 (SH2) domain (APS) and SH2-B enhance insulin-receptor autophosphorylation, extracellular-signal-regulated kinase and phosphoinositide 3-kinase-dependent signalling. *Biochem. J.* 371:405–412. doi:10.1042/BJ20021589

Alford, A.I., C.R. Jacobs, and H.J. Donahue. 2003. Oscillating fluid flow regulates gap junction communication in osteocytic MLO-Y4 cells by an ERK1/2 MAP kinase-dependent mechanism small star, filled. *Bone.* 33:64–70. doi:10.1016/S8756-3282(03)00167-4

Allen, H.L., A. Wase, and W.T. Bear. 1980. Indomethacin and aspirin: effect of nonsteroidal anti-inflammatory agents on the rate of fracture repair in the rat. *Acta Orthop. Scand.* 51:595–600. doi:10.3109/17453678008990848

Asahara, T., T. Murohara, A. Sullivan, M. Silver, R. van der Zee, T. Li, B. Witzenbichler, G. Schatteman, and J.M. Isner. 1997. Isolation of putative progenitor endothelial cells for angiogenesis. *Science*. 275:964–967. doi:10.1126/science.275.5302.964

Bilbe, G., E. Roberts, M. Birch, and D.B. Evans. 1996. PCR phenotyping of cytokines, growth factors and their receptors and bone matrix proteins in human osteoblast-like cell lines. *Bone*. 19:437–445. doi:10.1016/S8756-3282(96)00254-2

Blau, H.M., T.R. Brazelton, and J.M. Weimann. 2001. The evolving concept of a stem cell: entity or function? *Cell*. 105:829–841. doi:10.1016/S0092-8674(01)00409-3

Broudy, V.C. 1997. Stem cell factor and hematopoiesis. *Blood*. 90:1345–1364.

Calvi, L.M., G.B. Adams, K.W. Weibrecht, J.M. Weber, D.P. Olson, M.C. Knight, R.P. Martin, E. Schipani, P. Divieti, F.R. Bringhurst, et al. 2003. Osteoblastic cells regulate the haematopoietic stem cell niche. *Nature*. 425:841–846 (see comment). doi:10.1038/nature02040

Colnot, C. 2009. Skeletal cell fate decisions within periosteum and bone marrow during bone regeneration. *J. Bone Miner. Res.* 24:274–282. doi:10.1359/jbmr.081003

Colnot, C.I., and J.A. Helms. 2001. A molecular analysis of matrix remodeling and angiogenesis during long bone development. *Mech. Dev.* 100:245–250. doi:10.1016/S0925-4773(00)00532-3

Dominici, M., C. Pritchard, J.E. Garlits, T.J. Hofmann, D.A. Persons, and E.M. Horwitz. 2004. Hematopoietic cells and osteoblasts are derived from a common marrow progenitor after bone marrow transplantation. *Proc. Natl. Acad. Sci. USA*. 101:11761–11766. doi:10.1073/pnas.0404626101

Ema, H., K. Sudo, J. Seita, A. Matsubara, Y. Morita, M. Osawa, K. Takatsu, S. Takaki, and H. Nakauchi. 2005. Quantification of self-renewal capacity in single hematopoietic stem cells from normal and Lnk-deficient mice. *Dev. Cell*. 8:907–914. doi:10.1016/j.devcel.2005.03.019

Fitau, J., G. Boulday, F. Coulon, T. Quillard, and B. Charreau. 2006. The adaptor molecule Lnk negatively regulates tumor necrosis factor-alpha-dependent VCAM-1 expression in endothelial cells through inhibition of the ERK1 and -2 pathways. *J. Biol. Chem.* 281:20148–20159. doi:10.1074/jbc.M510997200

Fukiage, K., T. Aoyama, K.R. Shibata, S. Otsuka, M. Furu, Y. Kohno, K. Ito, Y. Jin, S. Fujita, S. Fujibayashi, et al. 2008. Expression of vascular cell adhesion molecule-1 indicates the differentiation potential of human bone marrow stromal cells. *Biochem. Biophys. Res. Commun.* 365:406–412. doi:10.1016/j.bbrc.2007.10.149

Harper, J., and M. Kalgsbrun. 1999. Cartilage to bone–angiogenesis leads the way. *Nat. Med.* 5:617–618. doi:10.1038/9460

Hassel, S., M. Yakymovych, U. Hellman, L. Ronnstrand, P. Knaus, and S. Souchelnytskyi. 2006. Interaction and functional cooperation between the serine/threonine kinase bone morphogenetic protein type II receptor with the tyrosine kinase stem cell factor receptor. *J. Cell. Physiol.* 206:457–467. doi:10.1002/jcp.20480

Horwitz, E.M., D.J. Prockop, L.A. Fitzpatrick, W.W. Koo, P.L. Gordon, M. Neel, M. Sussman, P. Orchard, J.C. Marx, R.E. Pyeritz, and M.K. Brenner. 1999. Transplantability and therapeutic effects of bone marrow-derived mesenchymal cells in children with osteogenesis imperfecta. *Nat. Med.* 5:309–313 (see comment). doi:10.1038/6529

Huang, X., Y. Li, K. Tanaka, K.G. Moore, and J.I. Hayashi. 1995. Cloning and characterization of Lnk, a signal transduction protein that links T-cell receptor activation signal to phospholipase C gamma 1, Grb2, and phosphatidylinositol 3-kinase. *Proc. Natl. Acad. Sci. USA*. 92:11618–11622. doi:10.1073/pnas.92.25.11618

Ii, M., H. Nishimura, A. Iwakura, A. Wecker, E. Eaton, T. Asahara, and D.W. Losordo. 2005. Endothelial progenitor cells are rapidly recruited to myocardium and mediate protective effect of ischemic preconditioning via "imported" nitric oxide synthase activity. *Circulation*. 111:1114–1120. doi:10.1161/01.CIR.0000157144.24888.7E

Jessop, H.L., S.C. Rawlinson, A.A. Pitsillides, and L.E. Lanyon. 2002. Mechanical strain and fluid movement both activate extracellular regulated kinase (ERK) in osteoblast-like cells but via different signaling pathways. *Bone*. 31:186–194. doi:10.1016/S8756-3282(02)00797-4

Karsenty, G., and E.F. Wagner. 2002. Reaching a genetic and molecular understanding of skeletal development. *Dev. Cell*. 2:389–406. doi:10.1016/S1534-5807(02)00157-0

Korbling, M., and Z. Estrov. 2003. Adult stem cells for tissue repair - a new therapeutic concept? *N. Engl. J. Med.* 349:570–582. doi:10.1056/NEJMra022361

Laing, A.J., J.P. Dillon, E.T. Condon, J.T. Street, J.H. Wang, A.J. McGuinness, and H.P. Redmond. 2007. Mobilization of endothelial precursor cells: Systemic vascular response to musculoskeletal trauma. *J. Orthop. Res.* 25:44–50. doi:10.1002/jor.20228

Li, Y., X. He, J. Schembri-King, S. Jakes, and J. Hayashi. 2000. Cloning and characterization of human Lnk, an adaptor protein with pleckstrin homology and Src homology 2 domains that can inhibit T cell activation. *J. Immunol.* 164:5199–5206.

Linden, M., A. Sirsjo, L. Lindbom, G. Nilsson, and A. Gidlof. 1995. Laser-Doppler perfusion imaging of microvascular blood flow in rabbit tenuissimus muscle. *Am. J. Physiol.* 269:H1496–H1500.

Liu, D., D.C. Genetos, Y. Shao, D.J. Geist, J. Li, H.Z. Ke, C.H. Turner, and R.L. Duncan. 2008. Activation of extracellular-signal regulated kinase (ERK1/2) by fluid shear is Ca(2+)- and ATP-dependent in MC3T3-E1 osteoblasts. *Bone*. 42:644–652. doi:10.1016/j.bone.2007.09.058

Manigrasso, M.B., and J.P. O'Connor. 2004. Characterization of a closed femur fracture model in mice. *J. Orthop. Trauma*. 18:687–695. doi:10.1097/00005131-200411000-00006

Marsh, D. 1998. Concepts of fracture union, delayed union, and nonunion. *Clin. Orthop. Relat. Res.*:S22–S30. doi:10.1097/00003086-199810001-00004

Matsumoto, T., A. Kawamoto, R. Kuroda, M. Ishikawa, Y. Mifune, H. Iwasaki, M. Miwa, M. Horii, S. Hayashi, A. Oyamada, et al. 2006. Therapeutic potential of vasculogenesis and osteogenesis promoted by peripheral blood CD34-positive cells for functional bone healing. *Am. J. Pathol.* 169:1440–1457. doi:10.2353/ajpath.2006.060064

Matsumoto, T., Y. Mifune, A. Kawamoto, R. Kuroda, T. Shoji, H. Iwasaki, T. Suzuki, A. Oyamada, M. Horii, A. Yokoyama, et al. 2008. Fracture induced mobilization and incorporation of bone marrow-derived endothelial progenitor cells for bone healing. *J. Cell. Physiol.* 215:234–242. doi:10.1002/jcp.21309

Mauch, P., C. Lamont, T.Y. Neben, C. Quinto, S.J. Goldman, and A. Witsell. 1995. Hematopoietic stem cells in the blood after stem cell factor and interleukin-11 administration: evidence for different mechanisms of mobilization. *Blood*. 86:4674–4680.

Nakamura, Y., F. Tajima, K. Ishiga, H. Yamazaki, M. Oshimura, G. Shiota, and Y. Murawaki. 2004. Soluble c-kit receptor mobilizes hematopoietic stem cells to peripheral blood in mice. *Exp. Hematol.* 32:390–396. doi:10.1016/j.exphem.2004.01.004

Nakazawa, T., A. Nakajima, N. Seki, A. Okawa, M. Kato, H. Moriya, N. Amizuka, T.A. Einhorn, and M. Yamazaki. 2004. Gene expression of periostin in the early stage of fracture healing detected by cDNA microarray analysis. *J. Orthop. Res.* 22:520–525. doi:10.1016/j.orthres.2003.10.007

Olmsted-Davis, E.A., Z. Gugala, F. Camargo, F.H. Gannon, K. Jackson, K.A. Kienstra, H.D. Shine, R.W. Lindsey, K.K. Hirschi, M.A. Goodell, et al. 2003. Primitive adult hematopoietic stem cells can function as osteoblast precursors. *Proc. Natl. Acad. Sci. USA*. 100:15877–15882. doi:10.1073/pnas.2632959100

Petite, H., V. Viateau, W. Bensaid, A. Meunier, C. de Pollak, M. Bourguignon, K. Oudina, L. Sedel, and G. Guillemin. 2000. Tissue-engineered bone regeneration. *Nat. Biotechnol.* 18:959–963 (see comment). doi:10.1038/79449

Rhee, S.T., L. El-Bassiony, and S.R. Buchman. 2006. Extracellular signal-related kinase and bone morphogenetic protein expression during distraction osteogenesis of the mandible: in vivo evidence of a mechanotransduction mechanism for differentiation and osteogenesis by mesenchymal precursor cells. *Plast. Reconstr. Surg.* 117:2243–2249. doi:10.1097/01.prs.0000224298.93486.1b

Rodriguez-Merchan, E.C., and F. Forriol. 2004. Nonunion: general principles and experimental data. *Clin. Orthop. Relat. Res.*:4–12. doi:10.1097/00003086-200402000-00003

Slack, J.M. 2000. Stem cells in epithelial tissues. *Science*. 287:1431–1433. doi:10.1126/science.287.5457.1431

Takahashi, T., C. Kalka, H. Masuda, D. Chen, M. Silver, M. Kearney, M. Magner, J.M. Isner, and T. Asahara. 1999. Ischemia- and cytokine-induced mobilization of bone marrow-derived endothelial progenitor cells for neovascularization. *Nat. Med.* 5:434–438. doi:10.1038/8462

Published September 20, 2010

Takaki, S., J.D. Watts, K.A. Forbush, N.T. Nguyen, J. Hayashi, J. Alberola-Ila, R. Aebersold, and R.M. Perlmutter. 1997. Characterization of Lnk. An adaptor protein expressed in lymphocytes. *J. Biol. Chem.* 272:14562–14570. doi:10.1074/jbc.272.23.14562

Takaki, S., K. Sauer, B.M. Iritani, S. Chien, Y. Ebihara, K. Tsuji, K. Takatsu, and R.M. Perlmutter. 2000. Control of B cell production by the adaptor protein lnk. Definition Of a conserved family of signal-modulating proteins. *Immunity.* 13:599–609. doi:10.1016/S1074-7613(00)00060-1

Takaki, S., H. Morita, Y. Tezuka, and K. Takatsu. 2002. Enhanced hematopoiesis by hematopoietic progenitor cells lacking intracellular adaptor protein, Lnk. *J. Exp. Med.* 195:151–160. doi:10.1084/jem.20011170

Takizawa, H., C. Kubo-Akashi, I. Nobuhisa, S.M. Kwon, M. Iseki, T. Taga, K. Takatsu, and S. Takaki. 2006. Enhanced engraftment of hematopoietic stem/progenitor cells by the transient inhibition of an adaptor protein, Lnk. *Blood.* 107:2968–2975. doi:10.1182/blood-2005-05-2138

Turner, A.M., L.G. Bennett, N.L. Lin, J. Wypych, T.D. Bartley, R.W. Hunt, H.L. Atkins, K.E. Langley, V. Parker, F. Martin, et al. 1995. Identification and characterization of a soluble c-kit receptor produced by human hematopoietic cell lines. *Blood.* 85:2052–2058.

Van Vlasselaer, P., N. Falla, H. Snoeck, and E. Mathieu. 1994. Characterization and purification of osteogenic cells from murine bone marrow by two-color cell sorting using anti-Sca-1 monoclonal antibody and wheat germ agglutinin. *Blood.* 84:753–763.

Wardell, K., A. Jakobsson, and G.E. Nilsson. 1993. Laser Doppler perfusion imaging by dynamic light scattering. *IEEE Trans. Biomed. Eng.* 40:309–316. doi:10.1109/10.222322

Weissman, I.L. 2000. Stem cells: units of development, units of regeneration, and units in evolution. *Cell.* 100:157–168. doi:10.1016/S0092-8674(00)81692-X

Wong, G.L., and D.V. Cohn. 1975. Target cells in bone for parathormone and calcitonin are different: enrichment for each cell type by sequential digestion of mouse calvaria and selective adhesion to polymeric surfaces. *Proc. Natl. Acad. Sci. USA.* 72:3167–3171. doi:10.1073/pnas.72.8.3167

Yokouchi, M., R. Suzuki, M. Masuhara, S. Komiya, A. Inoue, and A. Yoshimura. 1997. Cloning and characterization of APS, an adaptor molecule containing PH and SH2 domains that is tyrosine phosphorylated upon B-cell receptor stimulation. *Oncogene.* 15:7–15. doi:10.1038/sj.onc.1201163

Zhang, J., C. Niu, L. Ye, H. Huang, X. He, W.G. Tong, J. Ross, J. Haug, T. Johnson, J.Q. Feng, et al. 2003. Identification of the haematopoietic stem cell niche and control of the niche size. *Nature.* 425:836–841. doi:10.1038/nature02041

DOI: 10.3727/096368910X550189
CT-0249 Accepted 12/03/2010 for publication in "*Cell Transplantation*"

Local Transplantation of G-CSF-Mobilized CD34$^+$ Cells in a Patient with Tibial Nonunion: A Case Report

Ryosuke Kuroda (kurodar@med.kobe-u.ac.jp) [1, 2*], Tomoyuki Matsumoto (matsun@m4.dion.ne.jp) [1, 2*], Masahiko Miwa (masahiko@med.kobe-u.ac.jp) [1, 2], Atsuhiko Kawamoto (akawamoto@cdb.riken.jp) [2, 3], Yutaka Mifune (m-ship@kf7.so-net.ne.jp) [1, 2], Tomoaki Fukui (tomoakifukui@yahoo.co.jp) [1, 2, 3], Yohei Kawakami (yohei_kawakami@hotmail.com) [1, 2, 3], Takahiro Niikura (neotaka29@neptune.livedoor.com) [1, 2], Sang Yang Lee (sangyang@beige.plala.or.jp) [1, 2], Keisuke Oe (keisuke-oe@mtf.biglobe.ne.jp) [1, 2], Taro Shoji (taro@lexus-sc.jp) [1, 2, 3], Tomoya Kuroda (kurtomforce@gmail.com) [1, 2, 3], Miki Horii (hmiki@fbri.org) [2, 3], Ayumi Yokoyama (a-yokoyama@fbri.org) [2, 3], Takayuki Ono (t-ohno@tri-kobe.org) [4], Yasushi Koibuchi (y.koibuchi@fbri.org) [5], Shin Kawamata (kawamata@fbri.org) [5], Masanori Fukushima (mfukushi@tri-kobe.org) [4], Masahiro Kurosaka (kurosaka@med.kobe-u.ac.jp) [1, 2], Takayuki Asahara (asa777@is.icc.u-tokai.ac.jp) [2, 3, 4, 6]

[1] Department of Orthopedic Surgery, Kobe University Graduate School of Medicine

[2] Department of Translational Research, Institute of Biomedical Research and Innovation

[3] Group of Vascular Regeneration Research, Institute of Biomedical Research and Innovation

[4] Translational Research Informatics Center, Kobe, Japan

CT-0249 Cell Transplantation Epub: submitted 08/17/2010, provisional acceptance 10/18/2010

[5] Foundation for Biomedical Research and Innovation, Kobe Japan

[6] Department of Regenerative Medicine Science, Tokai University School of Medicine

* The first 2 authors contributed equally to this work.

Running title: $CD34^+$ Cell Transplantation for Tibial Nonunion

Word count: 1487 words

Address correspondence and reprint requests to

Ryosuke Kuroda, MD

Department of Orthpaedic Surgery,

Kobe University Graduate School of Medicine,

7-5-2 Kusunoki-cho, Chuo-ku, Kobe, 650-0017 Japan,

Phone: +81-78-382-5985, Fax: +81-78-351-6944

E-mail: kurodar@med. kobe-u.ac.jp

CT-0249 Cell Transplantation Epub: submitted 08/17/2010, provisional acceptance 10/18/2010

Abstract

Although implantation of crude bone marrow cells has been applied in a small number of patients for fracture healing, transplantation of peripheral blood $CD34^+$ cells, the hematopoietic/ endothelial progenitor cell-enriched population, in patients with fracture has never been reported. Here, we report the first case of tibial nonunion receiving autologous, granulocyte colony stimulating factor mobilized $CD34^+$ cells accompanied with autologous bone grafting. No serious adverse event occurred, and the novel therapy performed 9 months after the primary operation resulted in bone union 3 months later without any symptoms including pain and gait disturbance.

Clinical trial registration number: UMIN000002993

Key words: tibial nonunion; peripheral blood $CD34^+$ cells; G-CSF

Introduction

Whereas most fractures typically heal, a significant proportion (5-10%) of fractures fail to heal and result in delayed union or persistent nonunion (17,24). Nonunion of the long bone is a common problem that can be disabling. Treatment may require multiple operative procedures, prolonged hospitalization, and years of disability until a union is obtained or an amputation is performed. Among several factors resulting in this failure, severe skeletal injuries consisting of fractures with a compromised blood supply have a high risk for leading to either delayed unions or established nonunions. An essential requirement for healing such intractable fractures is to restore the local blood flow, which has traditionally been accomplished through complex vascular procedures or soft tissue transfers with adequate blood supply (8,10,21).

Recent progress in human embryonic and adult stem cell research have been reported in various fields, and bone formation and regeneration has received much attention as a target for regenerative medicine because of the capacity of stem cells to self-renew and differentiate into various types of adult cells or tissues (1,22,28). Adult human peripheral blood (PB) $CD34^+$ cells contain intensive endothelial progenitor cells (EPCs) as well as hematopoietic stem cells (HSCs) (3). Tissue ischemia and cytokine mobilize EPCs from BM into PB, and mobilized EPCs specifically home to sites of nascent neovascularization and differentiate into mature endothelial cells (vasculogenesis) (2,25). Therapeutic potential of BM-derived CD34+ cells for neovascularization in hindlimb, myocardial and cerebral ischemia has been demonstrated in both preclinical and clinical studies (12,16). Interestingly, recent

CT-0249 Cell Transplantation Epub: submitted 08/17/2010, provisional acceptance 10/18/2010

reports indicate that BM-derived CD34+ cells are capable of differentiating into osteogenic as well as hematopoietic and vasculogenic lineages (4,6,7,15,26). We and other groups reported that fracture induces mobilization of EPCs from BM into PB and incorporation of the circulating EPCs into the fracture site (13,14,19). We first demonstrated that systemic infusion of human circulating $CD34^+$ cells into immunodeficient rats with non-healing fracture contributes to morphological and functional fracture healing by enhancing vasculogenesis and osteogenesis (18). In addition, we attempted local transplantation of CD34+ cells with atelocollagen gel, a bio-absorbable scaffold, in the same animal model and demonstrated the similar effect at the lower dose compared with the systemic administration (20). Considering the essential scarcity of EPCs in adult human, this preclinical outcome provided us with a realistic strategy for the future clinical application.

Based on these scientific evidences, we here report the first clinical case of tibial nonunion treated with autologous, granulocyte colony stimulating factor (G-CSF) mobilized $CD34^+$ cells with atelocollagen scaffold immediately after the autologous bone grafting from iliac crest.

Case Report

A 42-year-old male presented himself at our hospital complaining of tibial delayed union with pain at the fracture site and disability of life. He had had a closed tibial fracture and been treated by open reduction and internal fixation with plate fixation at another hospital 9 months before the initial presentation at our hospital. During the 9 months, fracture site failed to heal in spite of treating with low intensity pulsed ultrasound device (Sonic Accelerated Fracture Healing System (SAFHS), Teijin Ltd., Japan). At the time of presentation, he complained of moderate pain and tenderness at the fracture site causing disability of weight bearing gait. He was clinically diagnosed as a nonunion according to the 1988 FDA Guidance Document Definition requiring 9 months duration of the non-united fracture with no evidence of progressive healing over the previous 3 months (27). Anteroposterior and lateral radiographs led to diagnosis of non-infected bone defect type nonunion showing no bridging of four cortical sides. The radiographs also revealed no apparent instability at the fracture site and absence of radiolucency around screws. The radiological findings were supported by 3-dimensional (3D) computed tomography (CT) (Fig. 1).

We obtained an informed consent from the patient for participating a phase I/ IIa clinical trial regarding transplantation of G-CSF mobilized $CD34^+$ cells in patients with nonunion. The clinical study protocol conformed to the Declaration of Helsinki and was approved by the ethics committees of the participating hospitals, Institute of Biomedical Research and Innovation (#08-01) and Kobe University Hospital (#735). After the subject eligibility was confirmed, the patient was registered as the first participant in the clinical trial. He received subcutaneous administration of G-CSF (5 μg/kg per day for 5

CT-0249 Cell Transplantation Epub; submitted 08/17/2010, provisional acceptance 10/18/2010

days) to mobilize EPCs from BM. Leukoapheresis (AS.TEC204; Fresenius HemoCare, Bad Homburg, Germany) was performed to harvest PB mononuclear cells (MNCs) on day 5. The apheresis product number was 2.85x 10^{10} cells and the frequency of $CD34^+$ cells in the apheresis product was 0.67% by fluorescence-activated cell sorting (FACS) analysis using CD34-specific monoclonal antibodies (Becton, Dickinson and Company, San Jose, CA). The apheresis product was kept at a concentration of ≤ 2 x10^8 cells/ml in autoplasma at 4 °C overnight ($\leq$18 hours) until the magnetic separation of $CD34^+$ cells was started. 1.30x 10^8 $CD34^+$ cells were isolated by the CliniMACS system consisting of a CliniMACS Instrument, CD34 reagent, phosphate-buffered saline/EDTA buffer, and tubing set (Miltenyi Biotec, Bergisch Gladbach, Germany). Purity of the isolated $CD34^+$ cells was 92.5% by FACS analysis and the cell viability was 98.3%. The sorted $CD34^+$ cells were also positive for the following endothelial lineage surface markers; CD133, c-Kit, and CD31 (94.8, 87.2, and 99.3%, respectively). Immediately after the magnetic cell sorting, a predefined dose (5 x 10^5 cells/ kg) of $CD34^+$ cells, which was determined by the pre-clinical study (20), was dissolved in 5 ml of atelocollagen gel (final concentration 1.5%) (KOKEN, Tokyo, Japan), which was used as a bio-absorbable scaffold for retaining the cells at the transplanted site.

Cell transplantation and bone grafting was performed under general anesthesia. Following refreshing fibrous tissue at the nonunion site and the surrounding cortical bone and grafting autologous cancellous bone from iliac crest, $CD34^+$ cells dissolved in atelocollagen gel were locally administered into the fracture site (bone defect site) using an injection needle under fluoroscopic control (Fig. 2). Replacement of the original plate was not performed because of no apparent instability at the fracture site and absence of radiolucency around screws.

The patient was allowed to gait with partial weight bearing at 6 weeks and with full weight bearing at 12 weeks after the operation. Twelve weeks after the treatment, the patient had no pain complaint with full weight bearing gait. Anteroposterior and lateral radiograph provided diagnosis of achieved union showing the bony bridging in three of four cortical sides. 3D-CT also supported the radiographical findings (Fig. 3). Taken together, the patient met the criteria of radiographical and clinical union as the primary end point in this treatment at 12 weeks. Six months after the treatment, the patient had no symptoms relating to the fracture and the combined therapy of cell transplantation and bone grafting. He could gait with full weight bearing. No serious adverse events relating to G-CSF administration, leukoapheresis and cell transplantation occurred during the observation period.

Discussion

To the best of our knowledge, this is the first clinical report of transplantation of autologous, G-CSF mobilized and purified $CD34^+$ cells in a patient with tibial nonunion. The cell therapy combined with autologous iliac bone grafting successfully achieved bone union, which was confirmed by clinical symptoms, radiograph and 3D-CT as early as 3 months after the treatment. As for the safety evaluation in the first case, there were no serious adverse events for which a causal relationship to the cell therapy could not be denied. In a recent clinical trial in our institution using autologous, G-CSF mobilized $CD34^+$ cells in 17 patients with critical limb ischemia (12), no serious adverse events occurred although mild to moderate events relating to G-CSF and leukoapheresis were frequent during the 12-week follow up. Safety, feasibility and efficacy of this cell-based therapy in patients with nonunion/delayed union would be evaluated after completing this phase I/IIa clinical trial.

Several research groups have demonstrated the usefulness of local transplantation of total BM cells for fracture healing (5,9). Hernigou et al reported that in 88% of patients with non-infected nonunions of the tibia, bone union was achieved by percutaneous grafting of autologous total BM cells accompanied with the external fixation or cast immobilization (9). Quarto et al are the first to report the clinical effectiveness and usefulness of BM mesenchymal stem cells (MSCs) associated to a porous ceramic for a large long-bone defects (23). Compared with transplantation of purified CD34+ cells, crude BM cell or BMMSC therapy does not require the time and cost for magnetic cell sorting. However, our group recently reported that

intramyocardial transplantation of human G-CSF mobilized, total MNCs represents a possible risk of severe hemorrhagic myocardial infarction through the excessive inflammation induced by abundant infiltration of hematopoietic cells (11). Infusion of the crude BM cells might cause similarly unfavorable event in the case of fracture. Further preclinical/ clinical studies would be warranted to compare the feasibility, safety and efficacy between the various modalities for bone repair.

In conclusion, harvest, isolation and transplantation of autologous, G-CSF mobilized $CD34^+$ cells was first performed in a patient with nonunion/delayed union. Both clinical and radiological healing of the fracture was achieved 12 weeks after the cell therapy and bone grafting. No serious adverse events occurred during the 12 week-follow up. These promising outcomes encourage the early completion of this phase I/ IIa clinical trial. Efficacy of the cell therapy would be further elucidated in a randomized controlled clinical trial with an appropriate control group receiving G-CSF only or placebo in the future.

Acknowledgements

We would like to thank Ms. Janina Tubby for her excellent editing assistance for preparing this manuscript. This study is partly supported by the grant of "Translation Research Support Program (2007-2012) of MEXT (Ministry of Education, Culture, Sports, Science and Technology) of Japan.

The authors declare no conflicts of interest.

References

1. Akiyama, M.; Nakamura, M. Bone regeneration and neovascularization processes in a pellet culture system for periosteal cells. Cell Transplant. 18:443-452; 2009.
2. Asahara, T.; Masuda, H.; Takahashi, T.; Kalka, C.; Pastore, C.; Silver, M.; Kearne, M.; Magner, M.; Isner, J. M. Bone marrow origin of endothelial progenitor cells responsible for postnatal vasculogenesis in physiological and pathological neovascularization. Circ. Res. 85:221-228; 1999.
3. Asahara, T.; Murohara, T.; Sullivan, A.; Silver, M.; van der Zee, R.; Li, T.; Witzenbichler, B.; Schatteman, G.; Isner, J. M. Isolation of putative progenitor endothelial cells for angiogenesis. Science 275:964-967; 1997.
4. Chen, J. L.; Hunt, P.; McElvain, M.; Black, T.; Kaufman, S.; Choi, E. S. Osteoblast precursor cells are found in CD34+ cells from human bone marrow. Stem Cells 15:368-377; 1997.
5. Connolly, J. F.; Guse, R.; Tiedeman, J.; Dehne, R. Autologous marrow injection as a substitute for operative grafting of tibial nonunions. Clin. Orthop. Relat. Res. 266:259-270; 1991.
6. Dominici, M.; Pritchard, C.; Garlits, J. E.; Hofmann, T. J.; Persons, D. A.; Horwitz, E. M. Hematopoietic cells and osteoblasts are derived from a common marrow progenitor after bone marrow transplantation. Proc. Natl. Acad. Sci. USA 101:11761-11766; 2004.
7. Ford, J. L.; Robinson, D. E.; Scammell, B. E. Endochondral ossification in fracture callus during long bone repair: the localisation of 'cavity-lining cells' within the cartilage. J. Orthop. Res. 22:368-375; 2004.
8. Gerstenfeld, L. C.; Cullinane, D. M.; Barnes, G. L.; Graves, D. T.; Einhorn, T. A. Fracture healing as a post-natal developmental process: molecular, spatial, and temporal aspects of its regulation. J. Cell. Biochem. 88:873-884; 2003.
9. Hernigou, P.; Poignard, A.; Beaujean, F.; Rouard, H. Percutaneous autologous bone-marrow grafting for nonunions. Influence of the number and concentration of progenitor cells. J. Bone Joint Surg. Am. 87:1430-1437; 2005.
10. Karsenty, G.; Wagner, E. F. Reaching a genetic and molecular understanding of skeletal development. Dev. Cell 2:389-406; 2002.
11. Kawamoto, A.; Iwasaki, H.; Kusano, K.; Murayama, T.; Oyamada, A.; Silver, M.; Hulbert, C.; Gavin, M.; Hanley, A.; Ma, H.; Kearney, M.; Zak, V.; Asahara, T.; Losordo, D. W. CD34-positive cells exhibit increased potency and safety for therapeutic neovascularization after myocardial infarction compared with total mononuclear cells. Circulation 114:2163-2169; 2006.
12. Kawamoto, A.; Katayama, M.; Handa, N.; Kinoshita, M.; Takano, H.; Horii, M.; Sadamoto, K.; Yokoyama, A.; Yamanaka, T.; Onodera, R.; Kuroda, A.; Baba, R.; Kaneko, Y.; Tsukie, T.; Kurimoto, Y.; Okada, Y.; Kihara, Y.; Morioka, S.; Fukushima, M.; Asahara, T. Intramuscular transplantation of G-CSF-mobilized CD34(+) cells in patients with critical limb ischemia: a phase I/IIa, multicenter, single-blinded, dose-escalation clinical trial. Stem Cells 27:2857-2864; 2009.
13. Laing, A. J.; Dillon, J. P.; Condon, E. T.; Street, J. T.; Wang, J. H.; McGuinness, A. J.; Redmond, H. P. Mobilization of endothelial precursor cells: systemic vascular response to musculoskeletal trauma. J. Orthop. Res. 25:44-50; 2007.
14. Lee, D. Y.; Cho, T. J.; Lee, H. R.; Park, M. S.; Yoo, W. J.; Chung, C. Y.; Choi, I. H. Distraction osteogenesis induces endothelial progenitor cell mobilization without inflammatory response in man. Bone 46:673-679; 2010.
15. Long, M. W.; Williams, J. L.; Mann, K. G. Expression of human bone-related proteins in the hematopoietic microenvironment. J. Clin. Invest. 86:1387-1395; 1990.
16. Losordo, D. W.; Schatz, R. A.; White, C. J.; Udelson, J. E.; Veereshwarayya, V.; Durgin, M.; Poh, K. K.; Weinstein, R.; Kearney, M.; Chaudhry, M.; Burg, A.; Eaton, L.; Heyd, L.; Thorne, T.; Shturman, L.; Hoffmeister, P.; Story, K.; Zak, V.; Dowling, D.; Traverse, J. H.; Olson, R. E.; Flanagan, J.; Sodano, D.; Murayama, T.; Kawamoto, A.; Kusano, K. F.; Wollins, J.; Welt, F.; Shah, P.; Soukas, P.; Asahara, T.; Henry, T. D. Intramyocardial transplantation of autologous CD34+ stem cells for intractable angina: a phase I/IIa double-blind, randomized controlled trial. Circulation 115:3165-3172; 2007.